J Mater Sci: Mater Electron (2017) 28:15495–15499
DOI 10.1007/s10854-017-7437-x

The effect of seed layer on optical and structural characteristics of ZnO nanorod arrays deposited by CBD method

Parisa Fallah Azad[1] · Nima Naderi[1] · Mohamad Javad Eshraghi[1] · Abouzar Massoudi[1]

Received: 20 May 2017 / Accepted: 29 June 2017 / Published online: 3 July 2017

Abstract ZnO nanorods were grown on p-type silicon by chemical bath deposition technique (CBD). ZnO nanorod arrays exhibited antireflective properties on silicon substrates. The ZnO nanorods structure, roughness characteristics of the film and phase were studied using field-emission scanning electron microscopy (FE-SEM), atomic force microscopy (AFM) and X-ray diffraction (XRD) while the optical properties were investigated by photoluminescence (PL) and reflectance spectrometery. XRD pattern indicated a sharp peak from (002) planes of ZnO. FESEM images indicated that the average diameter and length of the ZnO nanorods were 61.27 nm and 1.22 µm, respectively. Photoluminescence spectra exhibited a strong UV peak due to near-band-edge (NBE) emission. ZnO layer can reduce the reflection of incident light from silicon surface, thus it can be assumed an antireflective layer on Si substrates. Low running cost, cheap materials and compatibility of industrial process make this structures attractive for industrial optoelectronic devices.

1 Introduction

Improving the efficiency, reducing and controlling the production and operation costs of terrestrial photovoltaic devices are important for the further development of the photovoltaic technologies [1]. One of the important ways to achieve high efficiency solar cells is to increase the solar cell optical absorption by light trapping [2]. Light trapping could be achieved by utilization of nanostructrues because the nanostructured have very large surface areas per unit volume therefore increase the generation rate of photocarriers [3, 4]. Figure 1 shows how nanostructures can improve light trapping schematically. Zinc oxide is an inexpensive material, with refractive index (n) around 2 at 600 nm. It has a direct wide bandgap of 3.37 eV at room temperature with an exaction binding energy of 60 meV [5, 6]. ZnO nanorods arrays have properties which make them suitable for use in many applicatios such as photodetectors [7], solar cells [8] and gas sensors [9]. In recent years, one–dimensional (1D) ZnO nanostructures have been synthesized by implementing various techniques such as physical vapour deposition [10], molecular beam epitaxy [11], electrospinning [12], sputtering [13], pulsed laser deposition [14] and chemical bath deposition (CBD) [15]. Among these methods, chemical bath deposition has many advantages such as use of low temperature media, inexpensive equipment and environmental friendliness. Although CBD technique is an advantegous method for fabrication of nanostructures, but the layers synthesized by this technique are not uniform. The reason is the difference between lattice constant of top layer and substrate. In this report, the uniformity of ZnO nanostructures was enhanced by applying a seed layer between substrate and nanostructures. The synthesized uniform ZnO nanorods which were grown by this technique showed an outstanding optical properties and therefore they can be used in optical and electrical devices.

2 Experimental

A highly-doped p-type silicon (100) wafer was used as substrate. The silicon surface was washed using a conventional RCA method to remove the particulate matters on the surface.

✉ Nima Naderi
n.naderi@merc.ac.ir

[1] Department of Semiconductors, Materials and Energy Research Center, Karaj, Iran

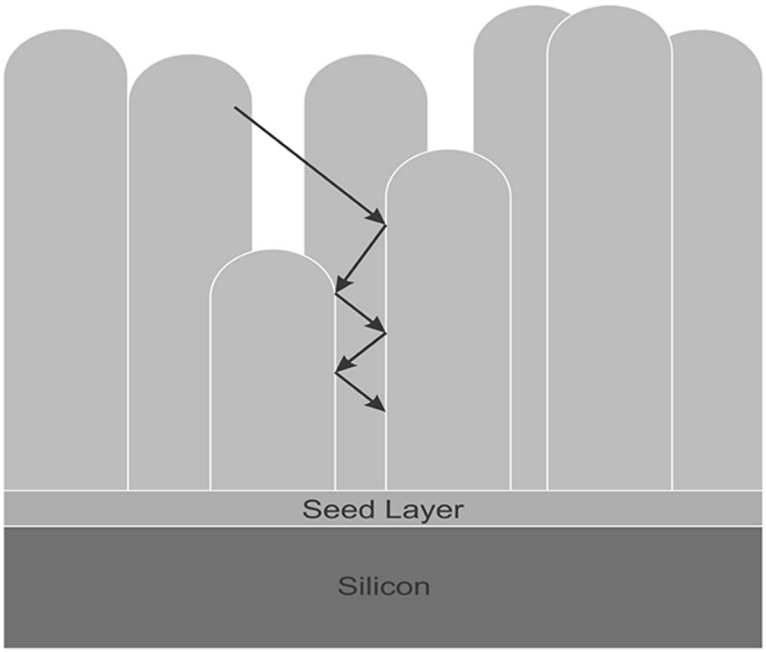

Fig. 1 Schematic of light trapping in ZnO nanorods/Si structure

Adopting the method, the substrates were successively dipped in 1:1:5 (by volume) of $NH_4OH:H_2O_2:H_2O$ for 10 min, 1:50 of $HF:H_2O$ for 20 s, and then in 1:1:6 of $HCl:H_2O_2:H_2O$ for another 10 min [16]. The samples were washed with deionized water and dried under an ambient nitrogen flow. ZnO thin film was deposited using RF magnetron sputtering system onto unheated Si (100) wafers (20 mm×20 mm) with a ZnO target (99.9% pure). The vacuum pressure in the process chamber was 6×10^{-4} torr and the working pressure was 6×10^{-2} torr. The target-to-substrate distance was chosen to be 50 mm. ZnO nanorod growth was performed by immersing samples in 1:10 (by volume) of zinc acetate dihydrate (Zn $((O_2CCH_3)_2(H_2O)_2)$) and ammonia (NH_4OH) for 120 min. The bath temperature was fixed at 85 °C. All of the chemicals were with high purity and were supplied from Merck, Germany.

3 Results and discussion

3.1 Chemical reactions for growth of ZnO nanorods using CBD technique

The following chemical reactions are carried out for synthesis of ZnO nanorods in chemical bath deposition technique [17]. Here, $Zn(CH_3COO)_2$ and ammonia (NH_4OH) provides Zn^{2+} and (OH^-) ions respectively. Therefore, two different complexes will appear. In order to facilitate nucleation and enhance growth rate of ZnO nanorods, a seed layer should be deposited on substrates. This will lead to growth of uniform and vertical ZnO nanorods.

$$Zn(CH_3COO)_2 \rightarrow Zn^{2+} + 2CH_3COO^-$$

$$NH_3 + H_2O \rightarrow NH_4 + OH^-$$

$$Zn^{2+} + 4OH^- \rightarrow [Zn(OH)_4]^{2-}$$

$$Zn^{2+} + 4NH_3 \rightarrow [Zn(NH_3)_4]^{2+}$$

$$Zn(NH_3)_4^{2+} + 2OH^- \rightarrow ZnO + 4NH_3 + H_2O$$

$$Zn(OH)_4^{2-} \rightarrow ZnO + H_2O + 2OH^-$$

In this process, many factors are effective for synthesis of high quality ZnO nanorods. One of the important parameters is concentration of ammonia which provides OH^- ions. High concentraion of negative OH^- ions can increase pH of solution which may result in precipitation of Zn^{2+} ions that hinders nucleation of ZnO nanorods [18].

3.2 Structure and morphology of ZnO nanorods

The sputtering parameters of ZnO seed layer are shown in Table 1. Figure 2. illustrates FE-SEM micrograph of ZnO nanorods. It shows that ZnO nanorods are grown vertically on seed layer. The size and shape of the nanostructure depend on time, temperature, concentration of solution, seed layer thickness and the pH of solution. The nanorods length and diameter are around 61.27 nm and 1.22 μm, respectively. It shows that ZnO nanorods are uniform, highly densed and they cover the entire surface, therefore this structure can enhance light absoption. Figure 3. shows XRD pattern of ZnO nanorods grown on ZnO seed layer which was sputtered on p-type silicon. Since the dominent peak is for (002) crystal plane, ZnO nanostructures were grown with this orientation. The formation energy of this

Table 1 Physical parameters related to RF magnetron sputtering of ZnO thin films on Si substrates

RF power	50 W
Substrate temperature	22 °C
Vacuum pressure	6×10^{-4} torr
Working pressure	6×10^{-2} torr
Deposition time	70 min
Target-substrate distance	50 mm

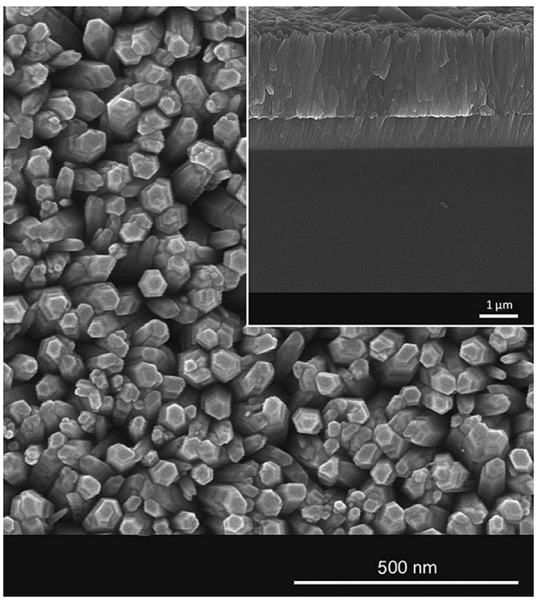

Fig. 2 FE-SEM of ZnO nanorods deposited on ZnO/Si substrate. The *inset* shows cross-sectional view of structure

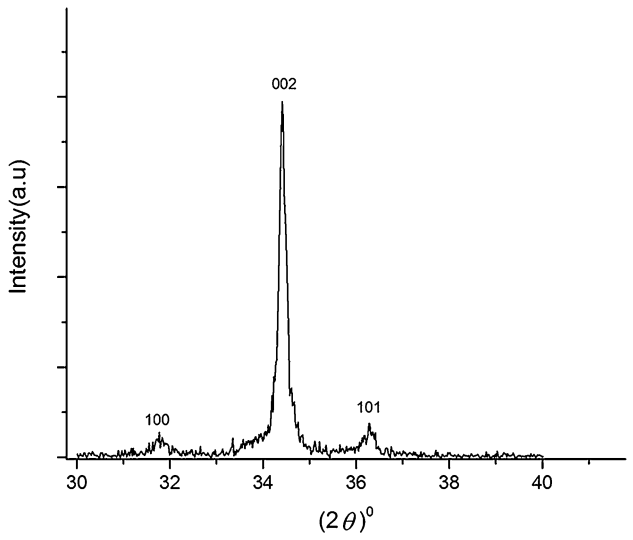

Fig. 3 XRD pattern of ZnO nanorods which were grown on ZnO seed layer using CBD technique

Table 2 Structural properties of ZnO nanorods on ZnO seed layer

(*hkl*)	2θ	*d*-spacing (Å)	FWHM (radian)	Crystallite size (nm)	Strain (%)
(100)	31.74	2.81	0.15	2.9	0.23
(002)	34.41	2.60	0.11	3.2	0.15
(101)	36.24	2.47	0.05	3.4	0.079

orientation is lower than other orientations in ZnO crystal, because the surface free-energy density of the (002) plane is lower than other orientations [19]. The lattice constant (*c*) of ZnO nanostructures along (002) orientation is calculated using Eq. 1 [20],

$$\frac{1}{d^2} = \frac{4}{3}\frac{h^2+hk+k^2}{a^2} + \left(\frac{l}{c}\right)^2 \quad (1)$$

The average crystallite size (*D*) of the ZnO nanostructures along the (002) peak is calculated by Scherrer equation [21]:

$$D = \frac{0.9\lambda}{\beta\cos\theta} \quad (2)$$

where *D*, θ, λ, and β represent the average crystallite size, Bragg diffraction angle, X-ray radiation wavelength, and full width at half maximum value (FWHM) of XRD peak, respectively. Table 2 summarizes the structural properties of deposited ZnO nanorods. The calculated average crystallite size of ZnO nanostructures was determined to be ~57 nm. Figure 4. shows EDX spectrum taken from ZnO nanorods. The chemical analysis of ZnO nanorods measured by EDX analysis shows the existence of zinc, oxygen and silicon atoms without the presence of any impurity in the structure. The Si peak is related to substrate. Therefore, EDX analysis indicates the high purity of sunthesized ZnO nanostructures. Atomic force microscopy (AFM) technique has been used for determining the surface roughness of ZnO nanorods (Fig. 5). The roughness of nanostructures was measured to be ~148 nm.

3.3 Optical properties of ZnO nanorods

Controlling the optical properties of different layers in a solar cell is very important for optimizing the efficieny of the device. Figure 6. shows a comparison between light reflectance from bare silicon, ZnO nanorads and ZnO thin films which were deposited on silicon substrate. The reflectance of bare silicon wafer is very higher than the other samples. ZnO nanorods layer showed low reflectance mainly in the visible region, which is important for solar cell application. Figure 7. illustrates the

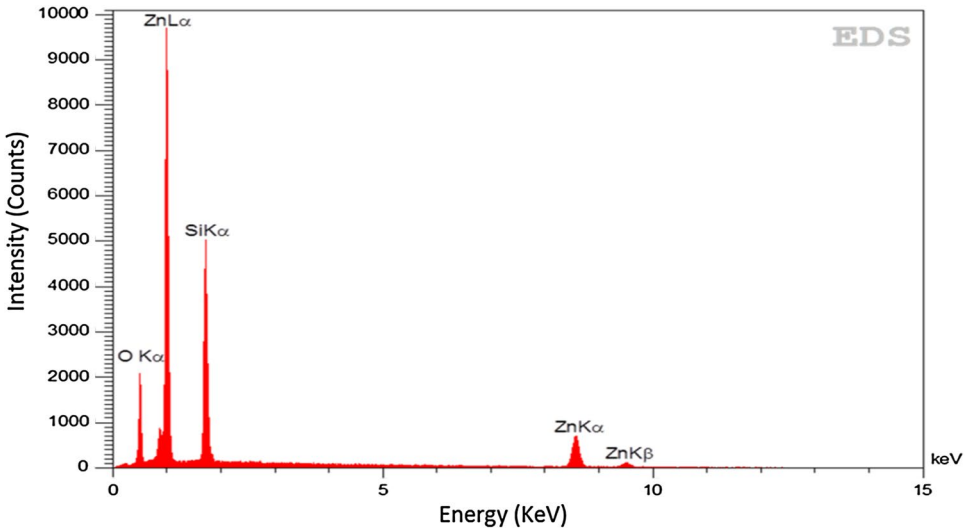

Fig. 4 EDX spectrum of ZnO nanorods grown on ZnO/Si substrate

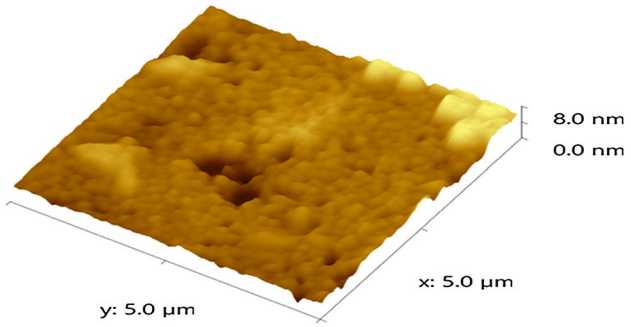

Fig. 5 Three–dimensional AFM micrograph of ZnO nanorods in the scale of 5×5 um^2

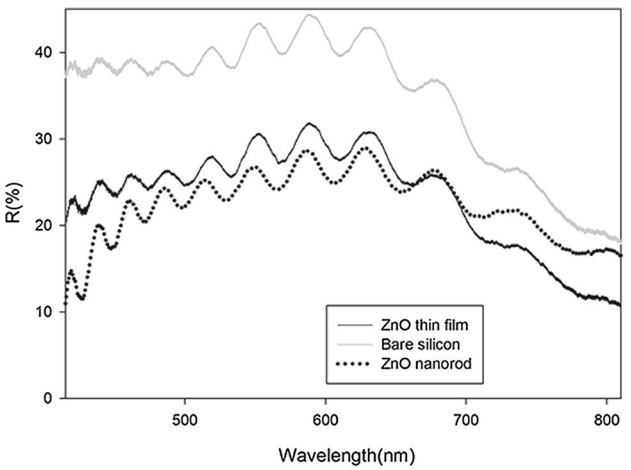

Fig. 6 Light reflectance spectra from polished silicon surface, ZnO thin film, and ZnO nanorods

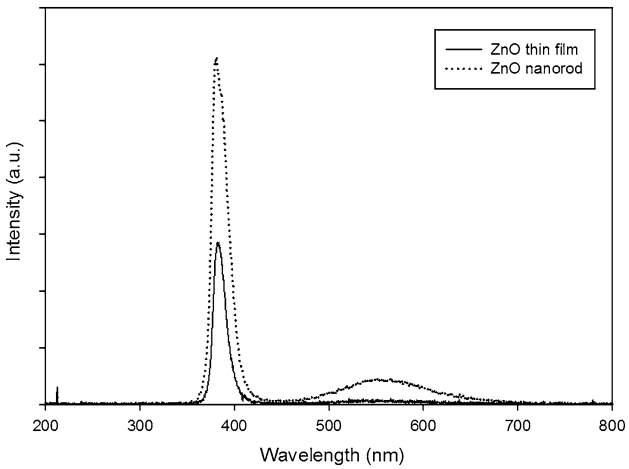

Fig. 7 Room-temperature PL spectra for ZnO nanorod arrays and ZnO thin film on silicon substrates

photoluminescence (PL) spectra of ZnO nanorods and ZnO thin film at the room-temperature. Two emission peaks are shown for both samples. For ZnO thin film, the first peak is at 382 nm and the second peak is at 556 nm. For ZnO nanorods, the first peak is at 379 nm and the second peak is at 554 nm. The highest intensity of PL peak is due to high amount of free excitons. The wide peak from 500 to 700 nm was related to deep-level emission of ZnO band gap, that was due to specific defects, such as oxygen vacancies and zinc interstitials .The intensity ratio of UV peak to visible peak was calculated to be 43.75 and 13.49 for ZnO thin film and nanorods, respectively. The high ratio of PL peak intensity is due to low amount of resident defects in ZnO crystal [22–24]. The photoluminescence properties of ZnO nanorods and ZnO thin film are summarized in Table 3.

Table 3 Photoluminescence properties of ZnO thin film and ZnO Nanorods

Sample	Peak position (nm)	FWHM (nm)	Intensity (a.u.)
ZnO thin film	382	13	5688
	556	69	130
ZnO nanorods	379	18	12,148
	554	95	900

4 Conclusion

We demonstrate a facile and inexpensive method for growth of ZnO nanostructures on the ZnO seed layer. The reflectance from ZnO nanorods is lower than polished silicon at wide wavelength range. The structure and morphology properties of ZnO nanorods were studied. XRD and FE-SEM results demonstrate that the ZnO nanorod arrays with a hexagonal wurtzite structure were grown densely and vertically on silicon. The PL spectrum showed a sharp peak related to UV emission and a broad green emission related to intrinsic defects. The results showed that ZnO seed layer facilitates nucleation of ZnO nanorods and enhances the uniformity of synthesized ZnO nanorods.

Acknowledgements This work was supported by Materials and Energy Research Center [Grant number: 471394052].

References

1. K.M.A. Saron, M.R. Hashim, N. Naderi, N.K. Allam, Sol. Energy **98**, 485–491 (2013)
2. N. Naderi, M.R. Hashim, J. Rouhi, H. Mahmodi, Mater. Sci. Semicond. Process. **16**, 542–546 (2013)
3. M. Petrov, K. Lovchinov, M. Mews, C. Leendertz, D. Dimova-Malinovska, JPCS **559**, 012018 (2014)
4. N. Naderi, M.R. Hashim, K.M.A. Saron, J. Rouhi, Semicond. Sci. Technol. **28**, 025011 (2013)
5. Q.X. Zhao, M. Willander, R.E. Morjan, Q.H. Hu, E.E.B. Campbell, Appl. Phys. Lett. **83**, 165–167 (2003)
6. V.V. Ursaki, O. Lupan, I.M. Tiginyanu, G. Chai, L. Chow, JNO. **6**, 473–477 (2011)
7. R. Shabannia, H.A. Hassan, H. Mahmodi, N. Naderi, H.R. Abd, Semicond. Sci. Technol. **28**, 115007 (2013)
8. P. Sudhagar, R.S. Kumar, J.H. Jung, W. Cho, R. Sathyamoorthy, J. Won, Y.S. Kang, Mater. Res. Bull. **46**, 1473–1479 (2011)
9. J. Xu, J. Han, Y. Zhang, Y.A. Sun, B. Xie, Sens. Actuators B **132**, 334–339 (2008)
10. B.D. Yao, Y.F. Chan, N. Wang, Appl. Phys. Lett. **81**, 757–759 (2002)
11. Y.W. Heo, V. Varadarajan, M. Kaufman, K. Kim, D.P. Norton, F. Ren, P. Fleming, Appl. Phys. Lett. **81**, 3046–3048 (2002)
12. D.D. Lin, H. Wu, W. Pan, Adv. Mater. **19**, 3968–3972 (2007)
13. W.T. Chiou, W.Y. Wu, J.M. Ting, Diam. Relat. Mater. **12**, 1841–1844 (2003)
14. J.I. Hong, J. Bae, Z.L. Wangand, R.L. Snyder, Nanotechnology **20**, 085609 (2009)
15. Z. Yang, Y.-Y. Shi, X.-L. Sun, H.-T. Cao, H.-M. Lu, X.-D. Liu, Mater. Res. Bull. **45**, 474–480 (2010)
16. N. Naderi, M.R. Hashim, Mater. Res. Bull. **48**, 2406–2408 (2013)
17. Y.-J. Lee, D.S. Ruby, D.W. Peters, B.B. McKenzie, J.W.P. Hsu, Nano Lett. **8**, 1501–1505 (2008)
18. T.H. Lee, H. Ryu, W.J. Lee, J. Alloys Compd. **597**, 85–90 (2014)
19. N. Naderi, M.R. Hashim, T.S.T. Amran, Superlattices Microstruct., **51**, 626–634 (2012)
20. O. Lupan, G. Chai, L. Chow, Microelectron. Eng. **85**, 2220–2225 (2008)
21. Y. Zhang, M.K. Ram, E.K. Stefanakos, D.Y. Goswami, J. Nanomater. **2012**, 20 (2012)
22. N. Naderi, M.R. Hashim, Mater. Lett. **97**, 90–92 (2013)
23. O.F. Farhat, M.M. Halim, M.J. Abdullah, M.K. Ali, N.K. Allam, Beilstein J Nanotechnol. **6**, 720–725 (2015)
24. Z. Khusaimi, M.H. Mamat, N. Abdullah, M. Rusop, Adv. Mater. Res. **667**, 86–92 (2013)